PROCEEDINGS OF SPIE

SPIEDigitalLibrary.org/conference-proceedings-of-spie

TiO₂ membranes for concurrent photocatalytic organic degradation and corrosion protection

Robert Liang, Melisa Hatat-Fraile, Horatio He, Maricor Arlos, Mark R. Servos, et al.

SPIE.

TiO_2 membranes for concurrent photocatalytic organic degradation and corrosion protection

Robert Liang*[a,b], Melisa Hatat-Fraile[c], Horatio He[a,b], Maricor Arlos[c], Mark. R. Servos[c], Y. Norman Zhou[a,b]

[a]Centre for Advanced Materials Joining, Department of Mechanical and Mechatronics Engineering, University of Waterloo, 200 University Avenue West, Waterloo, ON, N2L 3G1, Canada
[b]Waterloo Institute for Nanotechnology, University of Waterloo, 200 University Avenue West, Waterloo, ON, N2L 3G1, Canada
[c] Department of Biology, University of Waterloo, 200 University Avenue West, Waterloo, ON, N2L 3G1, Canada

ABSTRACT

Organic contaminants and corrosion in water treatment effluents are a current global problem and the development of effective methods to facilitate the removal of organic contaminants and corrosion control strategies are required to mitigate this problem. TiO_2 nanomaterials that are exposed to UV light can generate electron-hole pairs, which undergo redox reactions to produce hydroxyl radicals from adsorbed molecular oxygen. They hydroxyl radicals are able to oxidize organic contaminants in water. This same process can be used in conjunction to protect metals from corrosion via cathodic polarization. In this work, TiO_2 nanomaterials were synthesized and electrophoretically deposited on conductive substrates to serve as films or membranes. An illuminated TiO_2 film on a conductive surface served as the photoanode and assisted in the cathodic protection of stainless steel (SS304) and the degradation of organic pollutants, in this case glucose. This proof-of-concept relied on photoelectrochemical experiments conducted using a potentiostat and a xenon lamp illumination source. The open-circuit potential changes that determine whether a metal is protected from corrosion under illumination was observed; and the electrical characteristics of the TiO_2 film or membrane under dark and arc lamp illumination conditions were also analyzed. Furthermore, the effect of organic contaminants on the photocathodic protection mechanism and the oxidation of glucose during this process were explored.

Keywords: TiO_2 nanomaterials, photocatalysis, organic degradation, solar, corrosion protection, water treatment
*rliang@uwaterloo.ca; phone: 519-888-4567 ext. 33326

1. INTRODUCTION

Stainless steel is an important material in industrial applications due to its excellent corrosion resistance. They are widely used as materials of construction and a protective passive film layer forms spontaneously on the surface of the metal giving it good corrosion resistance; however passive film breakdown and localized corrosion in chloride-containing aqueous environments is a concern. Various surface treatments and coatings have been used to improve the corrosion resistance of stainless steels and other metals by providing a physical barrier between the environment and the metal surface [1]. However, these coatings can be easily scratched so cathodic protection systems are often used.

Cathodic protection is used to supply metal to be protected with electrons to shift its potential to a region where it is immune based on the Pourbaix diagram of the metal. The source of electrons could be supplied via sacrificial anode or impressed current using an external power supply. Sacrificial anodes, such as Mg and Zn, have a greater negative reduction potential compared to the metal being protected causing the anode to be consumed and replaced periodically [2]. The photocathodic protection method is a solution to replace sacrificial anodes with a semiconductor photoanode that generates photo-electrons under illumination. TiO_2 photoanodes that are connected to metals can drastically shift to negative potentials under illumination and such approach is effective to protect the cathode [3]. However, a plain TiO_2 coating usually suffers from charge recombination problems and is non-active under visible light illumination and in the dark.

Nanophotonic Materials XII, edited by Stefano Cabrini, Gilles Lérondel, Adam M. Schwartzberg, Taleb Mokari,
Proc. of SPIE Vol. 9545, 95450M · © 2015 SPIE · CCC code: 0277-786X/15/$18 · doi: 10.1117/12.2188466

The photoresponse of TiO_2 can be vastly improved. Many efforts have been made to enhance the performance of TiO_2 under UV and visible light illumination. It has been shown that metal nanoparticles (NPs), such as gold (Au), silver (Ag), platinum (Pt), and palladium (Pd), can be embedded in TiO_2 and enhance the photocatalytic activity of TiO_2 in visible light [4-7]. Ag NPs is often used because of its use in various applications and is cheaper alternative than noble metal elements [8]; however Ag is chemically reactive and will form a passivating oxide layer [9], but can be coated with a thin, transparent passive layer material (i.e. SiO_2) to prevent oxidation.

In this work, $Ag@SiO_2$-TiO_2 (AST) nanoparticles were mixed into a commercial TiO_2 powder and electrophoretic deposited on fluoride tin oxide (FTO) conductive glass substrates to serve as photoanodes. The morphology and elemental map of the composite thin films were characterized and the effects of AST on the photoelectrochemical (PEC) properties were examined. An illuminated photoanode assisted in the cathodic protection of SS304 and degradation of glucose.

2. MATERIALS AND METHODS

2.1 Materials

Fluoride tin oxide coated glass (FTO, surface resistivity, 15 ohm cm^{-2}), iodine, and acetylacetone was purchased for Sigma-Aldrich. Ti metal sheet (grade 2) was purchased at McMaster Carr.

2.2 Sample Preparation

2.2.1 Preparation of photoanodes

1% $Ag@SiO_2$-TiO_2/P25 composites (AST-P25) were made by mixing 990 mg of P25 and 10 mg of synthesized $Ag@SiO_2$-TiO_2 nanoparticles [10] in a 20 mL scintillation vial. 10 mL of ethanol was pipetted into the vial and the mixture was sonicated for 30 min. The AST-P25 solution was then placed in a beaker containing an electrophoretic solution mixture (140 mL ethanol, 100 mL methanol, 4 mL acetylacetone, 2 mL water, and 27 mg iodine). An electrophoretic setup was used to deposit the charged particles in the electrophoretic solution mixture. FTO glass was used as the cathode and Ti metal sheet (grade 2) was used as the anode. A DC power supply was used to supply a constant voltage of 30 V for 20 s. An average of 4.0 mg +/- 0.2 mg of the AST-P25 was deposited onto the FTO substrates. The FTO substrates were heat treated at 450°C to improve adhesion of the particles and remove organic impurities.

2.2.2 Preparation of SS304 working electrodes

SS304 sheet metal was cut into 9x9 mm squares using a hydraulic shear. The samples were progressively ground with 600, 800, and 1200 fine grit silicon carbide paper then polished for a mirror-like finish on a polishing pad using 1 μm diamond spray under 250 rpm rotation. Cleaned SS304 samples were placed in a working electrode cell when required to be used in PEC studies.

2.3 Material Characterization

The morphology of the as-synthesized samples was evaluated using a ZEISS LEO 1550 FE-SEM at an accelerating voltage of 10 kV. HRTEM observation was conducted using a JEOL 2010F at the Canadian Centre for Electron Microscopy (Hamilton, Ontario, Canada). The TEM samples were prepared by suspending TiO_2 nanomaterials in ethanol and drip casting the solution onto lacey carbon grids. The images were processed using Gatan Microscopy Suite: Digital Micrograph™ (Ver. 2.11.1404.0) and/or ImageJ. EDS maps were collected for AST nanoparticles and the Ag, Si, and Ti locations were superimposed on one image.

2.4 Photoelectrochemical Tests

Two PEC setups were used for the (i) PEC properties of photoanodes and (ii) corrosion performance of SS304 using photoanode assisted cathodic protection. For both setups, a xenon solar simulator (Newport, Research Solar Simulator) and a Gamry Potentiostat (Series 300) were used. All potentials were reported with respect to the saturated calomel electrode (V_{SCE}) or Ag-AgCl ($V_{Ag/AgCl}$). The photocurrent density tests were conducted at a constant potential of -0.3 V

vs. Ag-AgCl to determine the photocurrent properties of the photoanodes. The corrosion performance of SS304 using photoanodes was determined using a galvanic cell consisting of a photoanode cell (PAC) and a corrosion cell (CC), as seen in Fig. 1. The AST-P25 in the PAC is connected with the stainless steel (SS304) in the CC. A salt bridge containing 1 M KCl is connected between the cells. The CC consists of SS304 working electrode, Pt counter electrode, and SCE as reference in 0.5 M NaCl. The PAC consists of FTO glass with TiO_2 in 0.2 M KOH + hole scavenger solution. The PEC setup was used to evaluate the open circuit potential (OCP) for 10 hours under intermittent and continuous illumination.

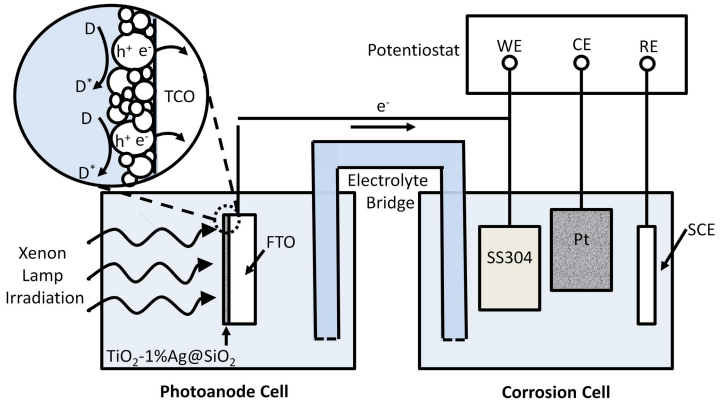

Figure 1: Schematic diagram of an electrochemical cell containing two compartments: (i) photoanode cell and (ii) corrosion cell.

3. RESULTS AND DISCUSSIONS

3.1 Materials Analysis

TEM images of as synthesized $Ag@SiO_2$-TiO_2 (AST) compounds and an SEM image of AST-P25 composite are shown in Fig. 2 and Fig. 3, respectively. The Ag nanoparticles developed using the polyol method are on average 60 nm as shown in Fig 2a. There is a thin layer of SiO_2 and TiO_2 around 10-15 nm Fig. 2b). The existence of Si (red) and Ti (green) elements in the superimposed STEM-EDX images (Fig. 2d) shows that there is evidence of a SiO_2-TiO_2 shell layer. The AST compound was mixed in P25 via sonication in ethanol solution. The resulting SEM image is shown in Fig. 3 where the P25 and AST nanoparticles are clustered together after mixing.

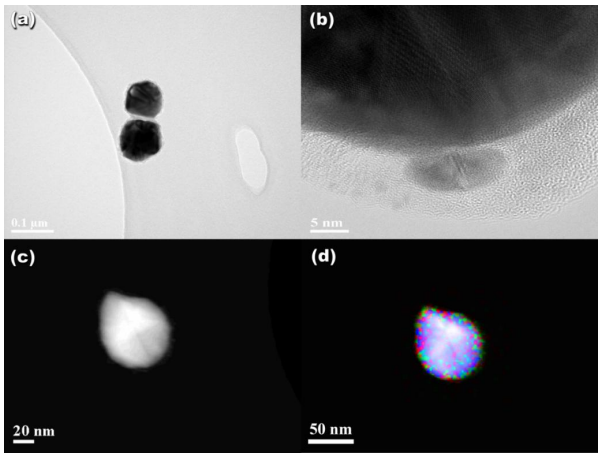

Figure 2: Images of as-synthesized AST nanoparticles in (a) conventional TEM, (b) HRTEM, (c) STEM, and (d) superimposed STEM-EDX (blue – Ag, red – Si, green – Ti)

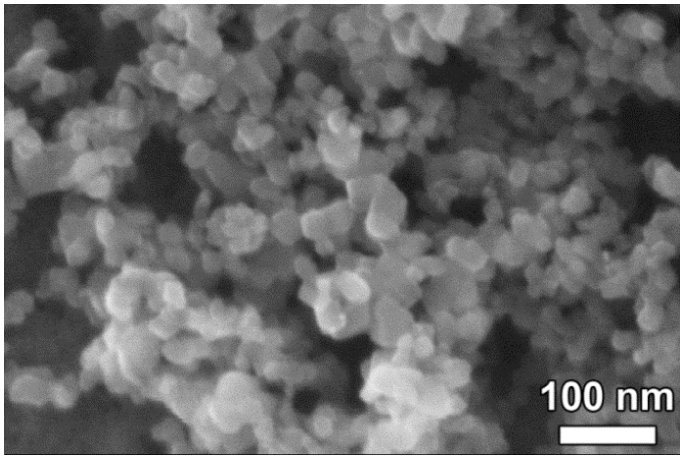

Figure 3: SEM image of AST-P25 composite

3.3 Photoelectrochemical Properties of AST-P25 Electrodes

3.3.1 Photocurrent densities under unfiltered and filtered lamp illumination

In Fig.4, the photocurrent density under unfiltered and filtered intermittent illumination was measured on P25 and AST-P25 electrodes. The photocurrent density of P25 and AST-P25 is 41 μm cm^{-2} and 84 μm cm^{-2}, respectively. Under filtered light, the photocurrent density of AST-P25 is 28 times the photocurrent density of P25. The use of Ag in TiO_2 improves the photocatalytic efficiency of TiO_2 under visible light due to the surface plasmons in Ag NPs [11].

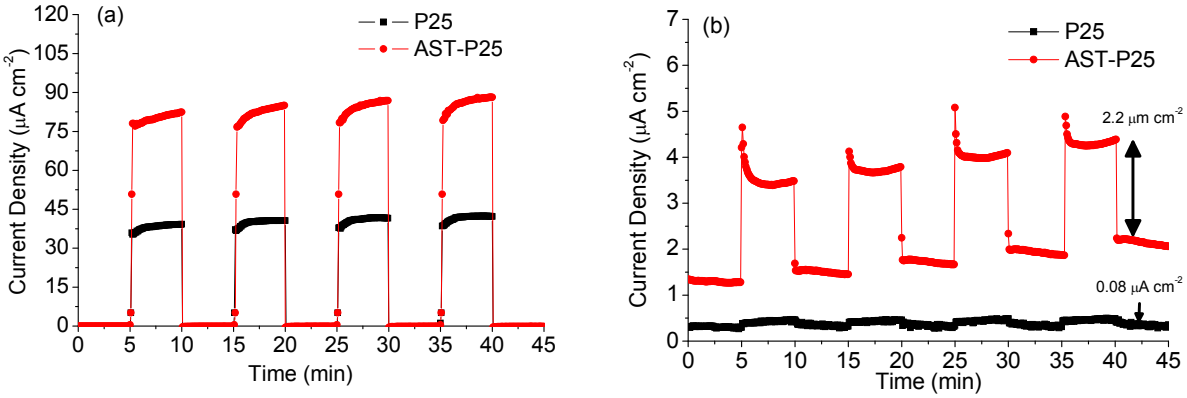

Figure 4: Photocurrent density tests using P25 and AST-P25 electrodes under (a) xenon lamp illumination and (b) filtered (400 nm cutoff filter) xenon lamp illumination in 1 M KOH solution.

3.3.2 Photocurrent densities as a function of glucose concentration

Glucose is used as a hole scavenger to reduce the recombination of the redox reaction. The photocurrent densities vs. glucose concentration curve obey Langmuir kinetics (Fig. 5). At lower concentrations, the process was limited by mass transfer. At higher concentrations, the photocurrent densities level off and the reaction rate was limited to interfacial reactions. The maximum photocurrent density is 620 μA cm^{-2} (50 mM glucose), 7.2 times the photocurrent density of 1 M KOH solution.

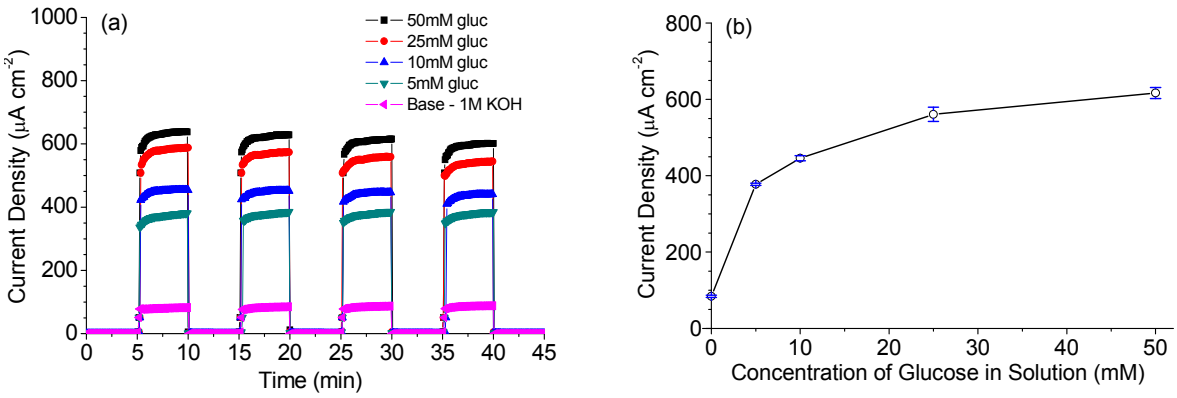

Figure 5: (a) Photocurrent density of AST-P25 electrodes in 1 M KOH electrolyte + glucose under intermittent illumination; (b) Photocurrent density as a function of glucose concentration in solution

3.3.3 Cathodic Protection of SS304 using AST-P25 Photoanodes – Open Circuit Potential

Glucose will oxidize into intermediate compounds under the TiO_2/UV advanced oxidation processes. The effect of glucose on the photocathode protection of SS304 is shown in Fig. 6 The PEC setup was used to evaluate the open circuit potential (OCP) and cyclic potentiodynamic polarization tests. The OCP test was carried out under open circuit (no current) mode for 10 hours under intermittent light and continuous illumination. Cyclic potentiodynamic polarization tests were conducted from -0.8 V_{SCE} to 0.8 V_{SCE} with a maximum current density of 20 mA cm^{-2}, in which polarization will reverse above this value. The test was performed at a scan rate of 0.167 mV s^{-1}.

The OCP shifts to more negative values and the magnitude of the shift is greater with the addition of glucose. Under intermittent light conditions and the addition of glucose, the SS304 is initially at an OCP of -0.25 V_{SCE} in the dark; when light is applied, there is an η of -0.73 V that decreases the coupled potential to -0.98 V_{SCE}. When light is removed, the potential of the coupled electrodes increases to -0.51 V_{SCE}; this suggests that SS304 is still partially protected from anodic reactions. The dark potential eventually decays to equilibrium, if the test was to be prolonged under dark conditions. After several intermittent light cycles, the η decreases in each cycle demonstrating that glucose is oxidized into less efficient hole scavengers.

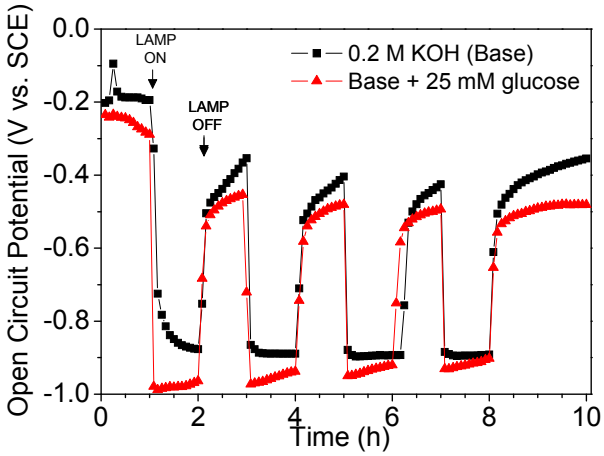

Figure 6: SS304 electrode coupled with an AST-P25 photoanode under intermittent light conditions using an electrolyte couple containing 0.5 M NaCl (corrosion cell) /1 M KCl (electrolyte bridge)/ 0.2 M KOH + 25 mM glucose (photoanode cell)

4. CONCLUSIONS

A PEC system employing TiO_2 photoanodes helped prevent steel corrosion by supplying photogenerated electrons to the SS304 cathode, while simultaneously oxidizing and converting the organic contaminant used. Conventional cathodic protection requires periodic replacement of sacrificial anodes or requires a constant supply of external power. A solar operated photocatalytic water treatment system alone, while possibly feasible in small-scale applications, is costly; adding corrosion protection functionality via cathodic polarization may make it justifiable to use. This proposed system is may consist of a flow-through photocatalytic reactor cell that degrades organic contaminants, while producing photo-electrons that can be used for the cathodic protection of steel structures.

REFERENCES

[1] Kraljić, M., Mandić, Z., and Duić, L., "Inhibition of steel corrosion by polyaniline coatings", Corrosion Science 45(1), 181-198 (2003).

[2] Jones, D.A., [Principles and Prevention of Corrosion, 9th ed.], Prentice Hall: Upper Saddle River, NH (1996).

[3] Tatsuma, T., Saitoh, S., Ohko, Y., and Fujishima, A., "TiO2-WO3 photoelectrochemical anticorrosion system with an energy storage ability," Chem. Mater. 13(9), 2838-2842, (2001).

[4] Hirakawa, T. and Kamat, P.V., "Charge separation and catalytic activity of Ag@ TiO2 core-shell composite clusters under UV-irradiation," J. Am. Chem. Soc. 127(11), 3928-3934 (2005).

[5] Yu, J., Qi, L., and Jaroniec, M., " Hydrogen production by photocatalytic water splitting over Pt/TiO2 nanosheets with exposed (001) facets," J. Phys. Chem. C 114(30), 13118-13125 (2010).

[6] Li, H., Bian, Z., Zhu, J., Huo, Y., Li, H., and Lu, Y., Mesoporous Au/TiO2 nanocomposites with enhanced photocatalytic activity. J. Am. Chem. Soc. 129(15), 4538-4539 (2007).

[7] Liang, R., Hu, A., Persic, J., and Zhou, Y.N., "Palladium Nanoparticles Loaded on Carbon Modified TiO_2 Nanobelts for Enhanced Methanol Electrooxidation.," Nano-Micro Lett. 5(3), 202-212 (2013).

[8] Butkus, M.A., Labare, M.P., Starke, J.A., Moon, K., and Talbot, M., " Use of aqueous silver to enhance inactivation of coliphage MS-2 by UV disinfection," Applied and environmental microbiology 70(5), 2848-2853 (2004).

[9] Awazu, K., Fujimaki, M., Rockstuhl, C., Tominaga, J., Murakami, H., Ohki, Y., Yoshida, N., Watanabe, T., "A plasmonic photocatalyst consisting of silver nanoparticles embedded in titanium dioxide," J. Am. Chem. Soc. 130(5), 1676-1680 (2008).

[10] Zhang, X., Zhu, Y., Yang, X., Wang, S., Shen, J., Lin, B., and Li, C., "Enhanced visible light photocatalytic activity of interlayer-isolated triplex $Ag@SiO_2@TiO_2$ core-shell nanoparticles, Nanoscale 5, 3359-3366 (2013).

[11] Pelaez, M., Nolan, N.T., Pillai, S.C., Seery, M.K., Falaras, P., Kontos, A.G.,....,and Dionysiou, D.D., " A review on the visible light active titanium dioxide photocatalysts for environmental applications," App.Catal. B: Environ.125, 331-349 (2012).